Exp. Theo. NANOTECHNOLOGY 10 (2026) 593-609 https://doi.org/10.56053/10.2.593

Expired Samafed drug as a nanotechnology-relevant corrosion inhibitor for carbon steel: Experimental and theoretical study

Shams A. Naji [1], *Rana Afif Anee* [2,3,*], *Sadeer M. Majeed* [4]

[1]Ministry of Environment, Baghdad, Iraq
[2]Department of Material Engineering, University of Technology– Iraq, Baghdad, Iraq
[3]Nanotechnology and Advanced Materials Research Center, University of Technology– Iraq, Baghdad, Iraq
[4]Department of Applied Sciences, University of Technology– Iraq, Baghdad, Iraq
[*]) Email: Dr.rana_afif@yahoo.com

Received 25/1/2026, *Received in revised form* 1/3/2026, *Accepted* 15/3/2026, *Published* 15/4/2026

All pharmaceuticals are unsafe after a certain period of time and may become medically toxic. However, they still contain active ingredients with chemical structures that can act as organic corrosion inhibitors and be used to protect various metallic materials. In this study, Samafed syrup, which contains Pseudoephedrine and Triprolidine, is investigated due to its ability to adsorb onto the surface of steel, thereby reducing corrosion. From a nanotechnology perspective, the adsorption of these organic molecules occurs at the nanoscale, leading to the formation of a protective nanolayer on the metal surface that enhances corrosion resistance. The inhibitor is applied at four concentrations (0.4, 2, 4, and 6 v/v%) and four temperatures (303, 313, 323, and 333 K) to evaluate polarization resistance and inhibition efficiency. The highest values of polarization resistance (5.49×10^{-3} Ω·cm²) and inhibition efficiency (92.02%) are obtained at 2 v/v% and 333 K. Surface characterization is performed using FTIR, which revealed the role of functional groups in the drug composition. Scanning electron microscopy (SEM) images showed improved surface coverage, while atomic force microscopy (AFM) analysis confirmed the formation of a uniform protective layer. AFM results further demonstrated nanoscale surface smoothing and the development of a compact nanostructured film formed by Fe–Samafed complexes. Theoretical calculations are conducted using adsorption isotherms and density functional theory (DFT). The results indicate that Samafed adsorption is predominantly physical in nature, supported by low adsorption/desorption constants and negative values of free energy, entropy, and enthalpy. Additionally, electronic property calculations confirmed the presence of active centers in the drug components capable of interacting with the steel surface. The findings highlight the importance of nanotechnology concepts in corrosion inhibition, where nanoscale adsorption and film formation play a key role in enhancing protective performance.

Keywords: Samafed drug; Corrosion inhibition; Adsorption isotherm; FTIR.

1. INTRODUCTION

The creation of a healthy environment with good quality of required life follows the strategies that address sustainability and equity with economic and social concerns [1-5]. The use of expired drugs as environmentally friendly corrosion inhibitors can realize the above principles due to the very low toxicity of drugs and the reduction of the accumulation of pharmaceutical waste, which can become toxic to microorganisms if disposed of in seawater [6-10]. For over ten years, outdated drugs have been used as inhibitors of various metallic materials in numerous electrolytes, with good efficiency [11, 12]. Researchers have focused their investigations on mixtures of organic molecules with multiple electron centers, including benzene rings, carbonyl, amino, and hydroxyl groups, as well as the presence of heteroatoms such as S, P, O, and N. Various drugs have been added [13–15] to protect steel, copper, aluminum, and other materials [16, 17]. Research has been conducted using the thermometric method, the geometric method, electrochemical impedance spectroscopy, potentiodynamic evaluation, the weight loss method, and the hydrogen evolution method supported by theoretical calculations [18-20].

In recent years, nanotechnology has played an important role in corrosion science, particularly in understanding surface interactions at the nanoscale [21-25]. The adsorption of inhibitor molecules on metal surfaces leads to the formation of protective nanolayers, which enhance corrosion resistance by improving surface coverage and reducing active corrosion sites. These nanoscale effects are critical in explaining the efficiency of organic inhibitors [26-30].

Samafed drug represents one of the over-the-counter drugs made in Iraq (SDI Samarra), which is used as an associated treatment for conditions such as allergies, common cold with cough, eye allergy, fever, influenza, headache, nasal congestion, and pain [31-35].

In the present work, Samafed with two components is used as an eco-friendly inhibitor to protect carbon steel in seawater electrolyte by adding four concentrations (0.4, 2, 4 and 6 v/v%) at four different temperatures (303, 313, 323 and 333 K) using electrochemical measurements supported by further theoretical calculations. Additionally, the study considers the nanoscale characteristics of the formed protective film, particularly through surface analysis techniques such as AFM and SEM, to better understand the inhibition mechanism.

2. EXPERIMENTAL MEASUREMENTS

2.1. Materials and chemicals

Carbon steel samples cut to the required dimensions (20 × 20 × 4 mm) served as the substrate. These samples are mounted with epoxy resin, then ground with SiC film and polished with Al_2O_3 paste for use in electrochemical experiments. Corrosive solution is prepared by dissolving 3.5 g of sodium chloride (from Loba Chemie PVT. LTD.) in 100 ml of distilled water to obtain simulated seawater. Samafed, produced by the National Pharmaceutical Company of Iraq (SDI Samarra), is used as an eco-friendly inhibitor after long-term storage and added at four concentrations (0.4, 2, 4 and 6 v/v%) at four different temperatures (303, 313, 323 and 333 K). The drug and its chemical formula are shown in Figure (1). The drug composition includes (1.25 mg) Triprolidine hydrochloride and (30 mg) Pseudoephedrine hydrochloride. At the molecular level, these organic components contain functional groups and heteroatoms that promote adsorption onto the metal surface, leading to the formation of a thin protective layer at the nanoscale, which is essential for corrosion inhibition.

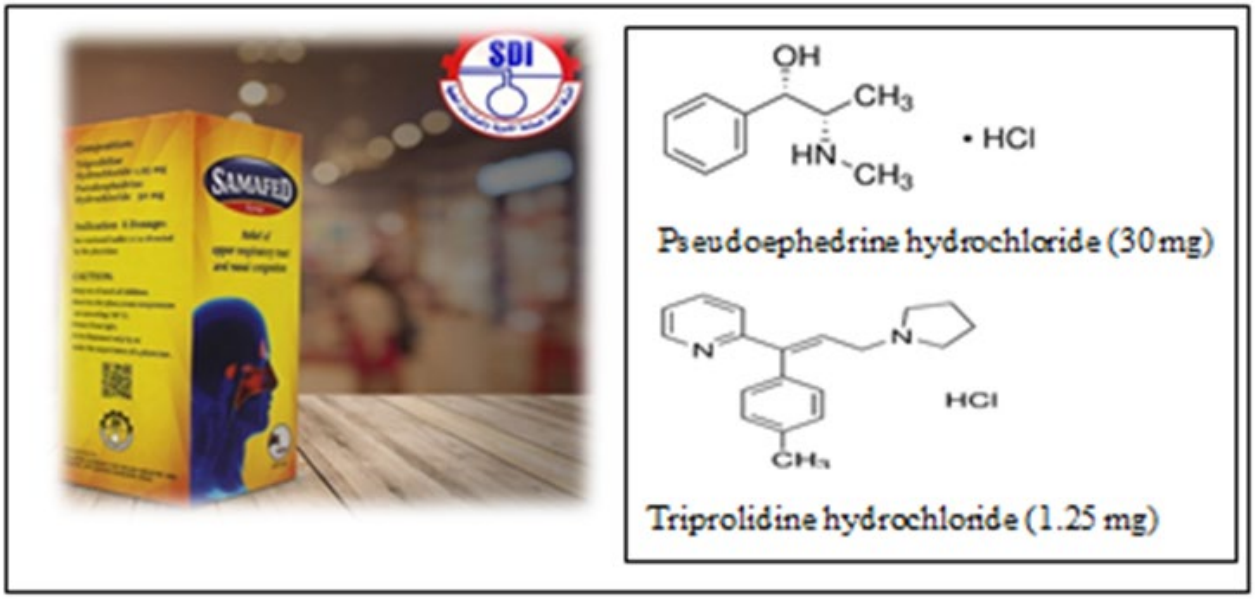

Figure 1 Used Samafed drug with its components.

2.2. Characterization tests

Different methods are used to evaluate the inhibited surface, including Fourier transform infrared spectroscopy (FTIR) from Bruker Company (ATR mode) and scanning electron microscopy (SEM) from TESCAN Company, which are used to examine the corroded and inhibited surfaces. Surface roughness and topography are measured using an atomic force microscope (AFM) (NaioAFM 2022, Nanosurf, Switzerland). AFM analysis is particularly important in nanotechnology studies, as it provides detailed information about surface morphology, roughness, and particle distribution at the nanometer scale, allowing for accurate evaluation of the formation of nanostructured protective films.

2.3.Electrochemical test

The main experimental test involved electrochemical measurements by recording the open circuit potential (Eoc) after 600 s of immersion, followed by recording the Tafel curves by applying ±0.2 V at a scan rate of 1 mV/s [31, 32]. These measurements are used to determine the corrosion potential (Ecorr), corrosion current density (icorr), and Tafel slopes for the cathodic (b_c) and anodic (b_a) reactions using a three-electrode jacket cell connected to a potentiostat (Corrtest, model CS350). These electrochemical parameters indirectly reflect the effectiveness of nanoscale adsorption of inhibitor molecules on the metal surface, which contributes to reducing corrosion reactions.

Theoretical Calculations

From corrosion data, inhibition parameters are calculated included the polarization resistance (R_p) as follow [33, 34]:

$$R_p = \frac{\boldsymbol{b_c \times b_a}}{\boldsymbol{2.303\, i_{corr}(b_c + b_a)}} \quad (1)$$

And by using current densities without drug (i_{corr}) and with drug (i'_{corr}), the inhibition efficiencies ($IE\%$) for used drug are also calculated as follow [35, 36]:

$$IE\% = \left[1 - \frac{i'_{corr}}{i_{corr}}\right] \times 100 \quad (2)$$

Adsorption isotherm calculation began from the coverage (θ) data that equal $\theta = (\frac{IE}{100})$ to apply Langmuir formula [37]:

$$\frac{C_{drug}}{\theta} = \frac{1}{K_{ads}} + C_{drug} \quad (3)$$

where (C_{drug}) is the concentration of added drug and (K_{ads}) is adsorption/desorption constant which is calculated (K_{ads}) either from intersection of Langmuir relation or directly as $K_{ads} = \frac{\theta}{C_{drug}(1-\theta)}$ at different temperatures. Thermodynamic functions including the apparent free adsorption energy (ΔG^{o}_{ads}) can be calculated according to the equation (4) [38] followed by calculating the entropy (ΔS^{o}_{ads}) and enthalpy (ΔH^{o}_{ads}) according to equations (5) and (6) [39]:

$$\Delta G^{o}_{ads} = -2.303\, RT(log\, 55.5\, \times K_{ads}) \quad (4)$$

$$\Delta S^{o}_{ads} = -\left[\frac{\partial(\Delta G^{o}_{ads})}{\partial T}\right] \quad (5)$$

$$\Delta G^{o}_{ads} = \Delta H^{o}_{ads} - T\Delta S^{o}_{ads} \quad (6)$$

The electronic calculations are predicted by quantum programs for Samafed components to show the sites related to inhibition role using $(Gaussian\ 09$, Revision D.01) [40] with basis set $(6-311G)$ [41, 42] as well as using the Becke three-parameter hybrid $(B3)$ [43] and the Lee-Yang-Parr (LYP) correlation functional $(B3LYP)$ [44].

Some theoretical data are calculated by density function theory (DFT) method using some formulas included Ionization potential (I) Electron affinity (A) in eq. (7); Hardness (η), Softness (σ), Electronegativity (χ) in eq. (8); Chemical potential (μ), Electrophilicity (ω) and Fraction of electrons transported (ΔN) are calculated according to in eq. (9) [45]:

$$I = -E_{HOMO}\ ,\quad A = -E_{LUMO} \quad (7)$$

$$\eta = \frac{I-A}{2}\ ,\ \sigma = \frac{1}{2\eta}\ ,\ \chi = \frac{I+A}{2} \quad (8)$$

$$\mu = -\chi,\ \omega = \frac{\chi^2}{2\eta},\ \Delta N = \frac{\chi_{Fe}-\chi_{Inh}}{2(\eta_{Fe}+\eta_{Inh})} \quad (9)$$

where E_{HOMO} is the highest occupied molecular orbital energies and (E_{LUMO}) the lowest unoccupied molecular orbital energies. These theoretical calculations provide insight into the nanoscale interaction between inhibitor molecules and the metal surface, helping to explain the adsorption mechanism and the formation of a stable protective nanolayer responsible for corrosion inhibition.

3. RESULTS AND DISCUSSION

3.1. Experimental findings

The corrosion behavior is the first test conducted to investigate the inhibitory role of any inhibitor. In current studies, carbon steel is dissolved at the anodic site to form ferrous ions (Fe^{2+}) by releasing electrons transferred to the cathode site to reduce oxygen molecules and form hydroxyl ions (OH^{-}). These two ions combine to form iron hydroxide in the following way:

$$Fe^{2+} + 2OH^{-} \rightarrow FeOH_2 \quad (10)$$

This hydroxide then oxidizes as passive film (Fe_2O_3), but the presence of chloride ions (Cl^-) attacks this passive film and destroys it to form iron chloride $FeCl_2$. The presence of any substance in a corrosive electrolyte with electron density can adsorb to the metal surface to reduce chloride attack. The addition of Samafed and its components shifted the polarization curves towards noble current densities at two lower temperature and toward active direction at two higher temperatures. All added

concentrations shifted the polarization curves towards lower current density values, approaching the inhibition efficiency and polarization resistance shown in Table (1). The data in table (1) shows that 2 v/v% is the best concentration among the other concentration that added, and the efficiencies are ranged from (59.56%) to (92.02%), depending on the chemical structure of components in the Samafed drug. Also, the highest resistance values are recorded for the concentration of 2 v/v% as ranged from 5.49×10-3 to 1.97×10^{-3} $\Omega.cm^2$ for temperature range of 333 to 303 K respectively. The second test that is carried out is the Fourier Transform Infrared Spectroscopy (FTIR) for Samafed drug as it is and for film formed on the steel surface in the presence of the best concentration 2 v/v%. Samafed drug is contain Pseudoephedrine hydrochloride (30 mg) and Triprolidine hydrochloride (1.25 mg). This drug gives FTIR spectrum as shown in Figure (3) which indicates the broad band at 3290 cm^{-1} related to $O-H$ stretching vibrations, and very small peak which can be seen at $\approx 2937 cm^{-1}$ is related to $N-H$ and $C-H$ stretching vibrations. followed by medium band at 1642 cm^{-1} related to $C=C$ and $C=O$ stretching vibrations and then at 1414 cm^{-1} corresponded to $C=C$ bond, also can be stretching of $C-N$ bond as small band at1335 cm^{-1}, After corrosion/ Inhibition process, the film formed on carbon steel substrate is liable to FTIR analysis for concentration of 2 v/v% to get the spectrum as in the same Fig (3) After adsorption the Samafed drug on metallic surface, the intensity of hydroxyl and carbonyl groups in addition to oxygen atom of ether is decreased that give indication that the attractive is done through these groups. Another inspection to confirm the inhibitory role of samafed drug is scanning electron microscopy Figure 4 The indentation of surface by SEM indicates the anodic and cathodic sites upon the corroded surface at two magnifications (100 μm & 10 μm) with clustering of corrosion product with imaging of surfaces for both corroded and inhibited ones as in Figure (4- i and ii), where in (i) the clustering of corrosion products produced by dissolution of metals at the anodic sites such as iron chlorides and damaged passive films with non-protective rust-like scales can be observed. (ii) After inhibition, the regular layer of adsorbed drug molecules is clear, resulting in good coverage and smoother surface. The two-dimensional and three-dimensional AFM analysis images indicate the topographies of the corroded and inhibited surfaces, confirming the appearance of galvanic cells for the corroded surface (Figure 5 (i)) and the clustering of drug molecules for the Samafed drug-inhibited surface (Figure 5 (ii)). In fig 6. The bulky molecules in drugs led to decrease the surface roughness from (270.8 nm) to (90.77 nm) for corroded and inhibited surface respectively. The adsorption of this bulk complex also affected the mean diameter calculation upon the surface as shown in Figure (6) which increased the mean diameter for particles from (56.42 nm) to (128.0 nm) for corroded and inhibited surface respectively, with 3D view of the surface confirming the decreases in the anodic sites (Blak colored region) compared with view of the inhibited surface. The surface volume parameters presented in Figure 6 indicate a reduction in void and pit volume after inhibition. The void volume decreased from 378.8 nm in the corroded samples to 159.0 nm in the inhibited samples, while the pit volume decreased from 44.70 nm to 8.869 nm, respectively.

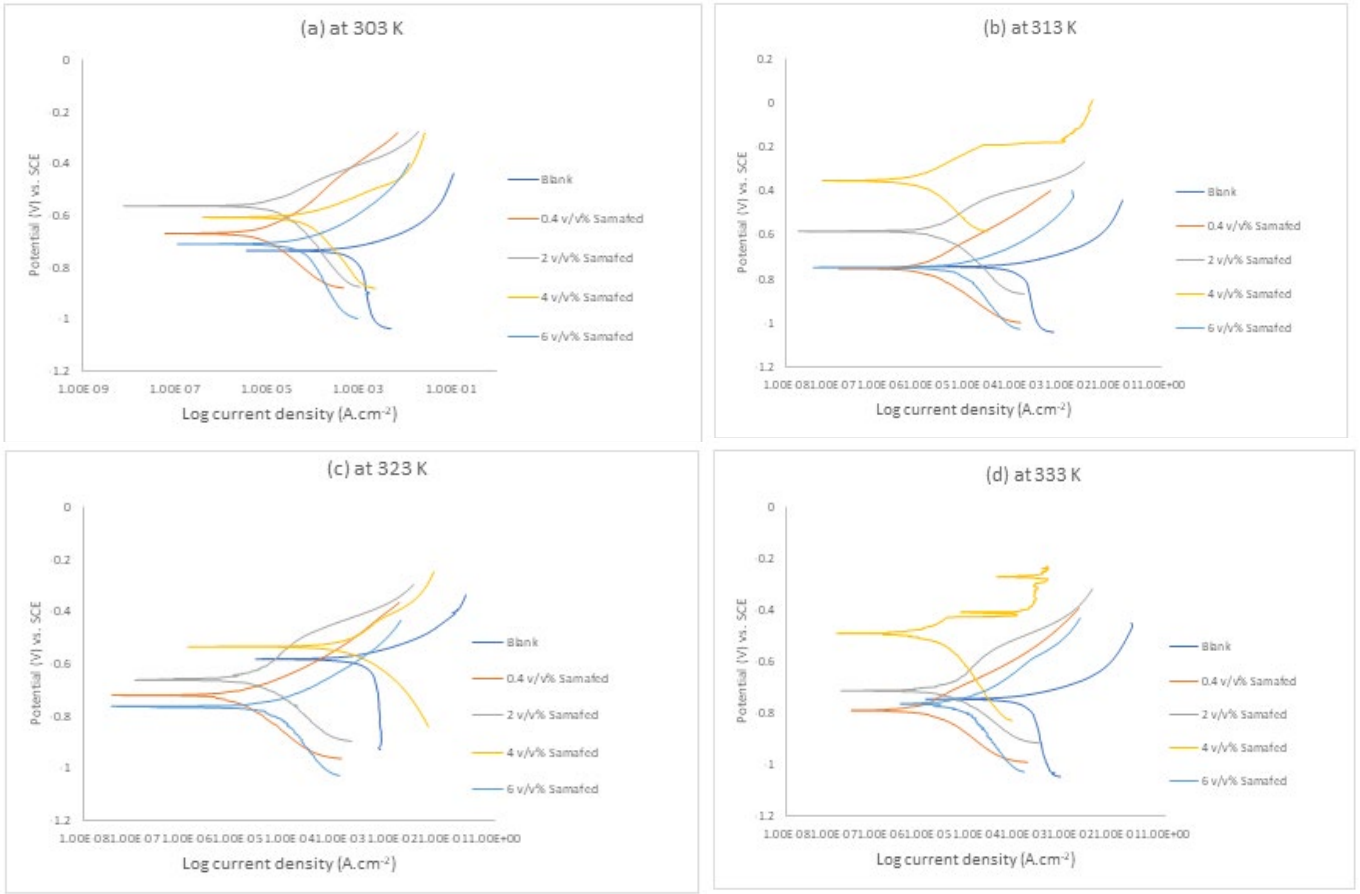

Figure 2 Tafel plots for inhibition by Samafed at four temperatures; (a) 303K, (b) 313K, (c) 323K and (d) 333K.

Table 1 Corrosion and inhibition data in the presence of four concentrations of Samafed drug.

Conc. (v/v%)	Temp. (K)	-E_{corr} (V)	i_{corr}*10^{-6} (A.cm^{-2})	-b_c (mV.dec^{-1})	+b_a (mV.dec^{-1})	$R_p \times 10^{-3}$ (Ω.cm^2)	IE (%)
Blank	303	0.735	18.17	84.56	71.055	0.92	---
	313	0.744	19.36	83.8	70.235	0.85	---
	323	0.581	21.67	39.1	76.846	0.51	---
	333	0.746	23.56	44.05	65.564	0.48	---
0.4	303	0.668	9.581	155.45	121.55	3.09	47.27
	313	0.752	8.871	126.39	129.39	3.12	54.17
	323	0.720	8.573	146.09	74.693	2.50	60.43
	333	0.790	5.172	50.437	94.065	2.75	78.04
2	303	0.562	7.347	60.483	74.799	1.97	59.56
	313	0.583	2.887	31.595	39.759	2.64	85.08
	323	0.661	2.271	13.955	26.102	1.73	89.52
	333	0.713	1.878	38.838	61.116	5.49	92.02
4	303	0.606	7.529	216.2	73.91	3.17	58.56
	313	0.352	6.421	138.08	119.22	4.32	66.83
	323	0.534	5.263	99.169	134.67	4.71	75.71
	333	0.490	2.844	19.282	40.765	1.99	87.92
6	303	0.709	7.172	340.8	99.821	4.67	60.52
	313	0.747	6.345	255.91	84.358	4.34	67.22
	323	0.763	5.223	8.6803	9.2606	0.37	75.89
	333	0.765	4.807	285.59	127.98	7.98	79.59

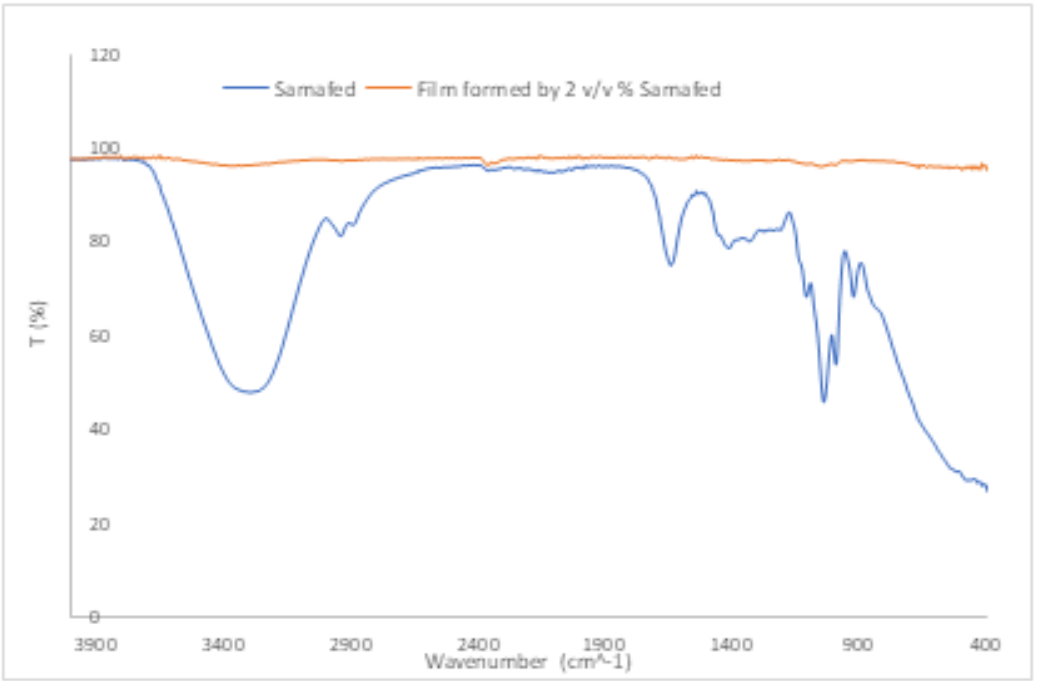

Figure 3 FTIR Spectra for Samafed drug as it is and film formed in inhibition process.

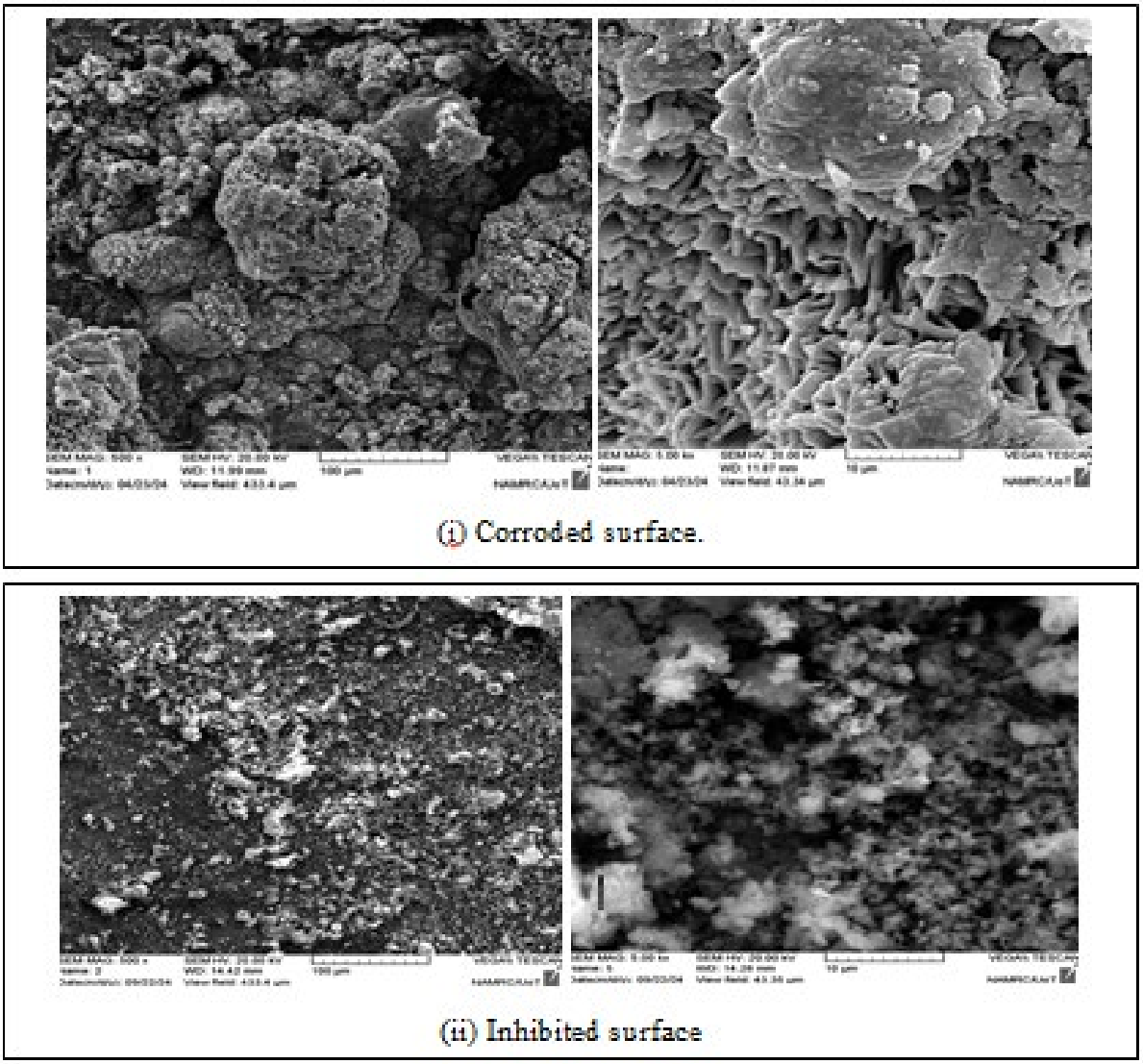

Figure 4 SEM images for corroded surface (i) and inhibited surface (ii) for Samafed drug at two magnifications.

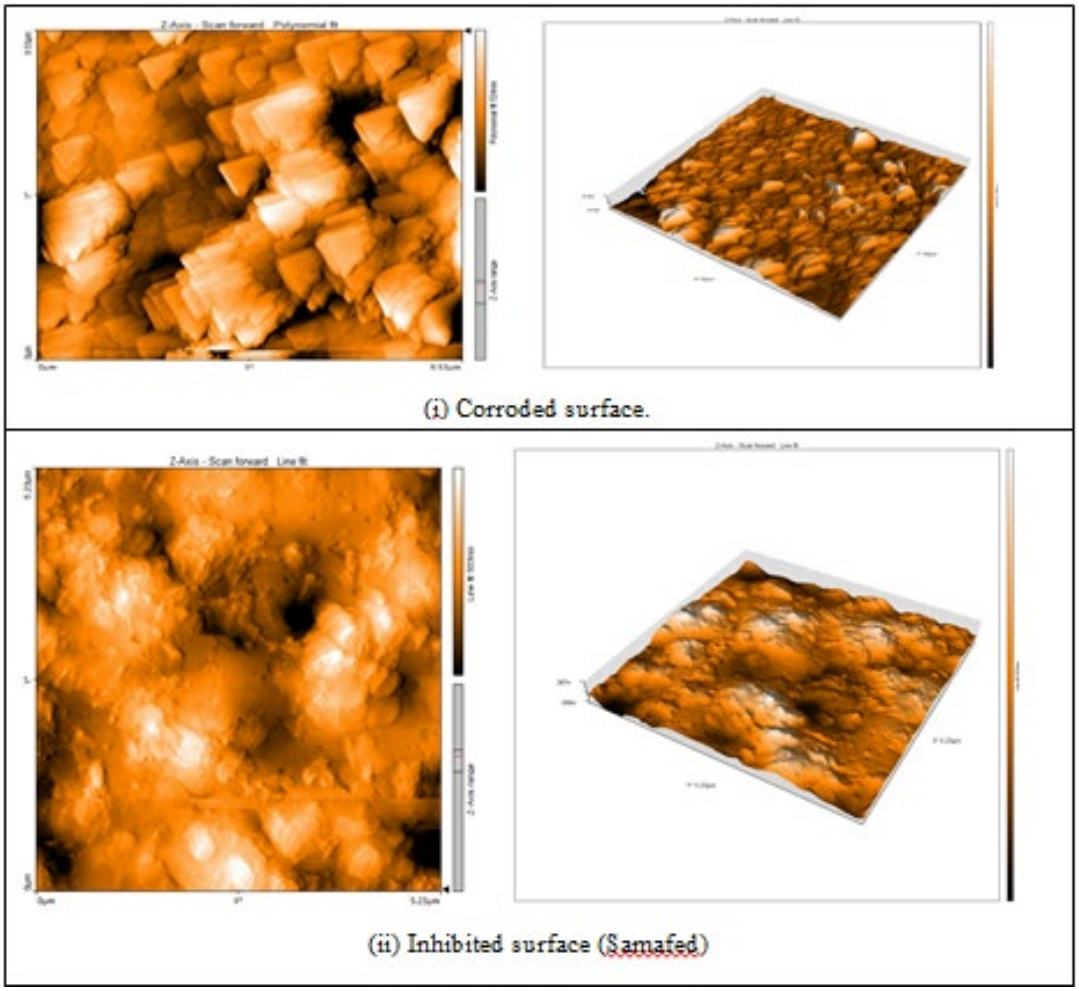

Figure 5 2*D* and 3*D* images for corroded surface (i) and inhibited surface (ii) For Samafed drug from AFM data.

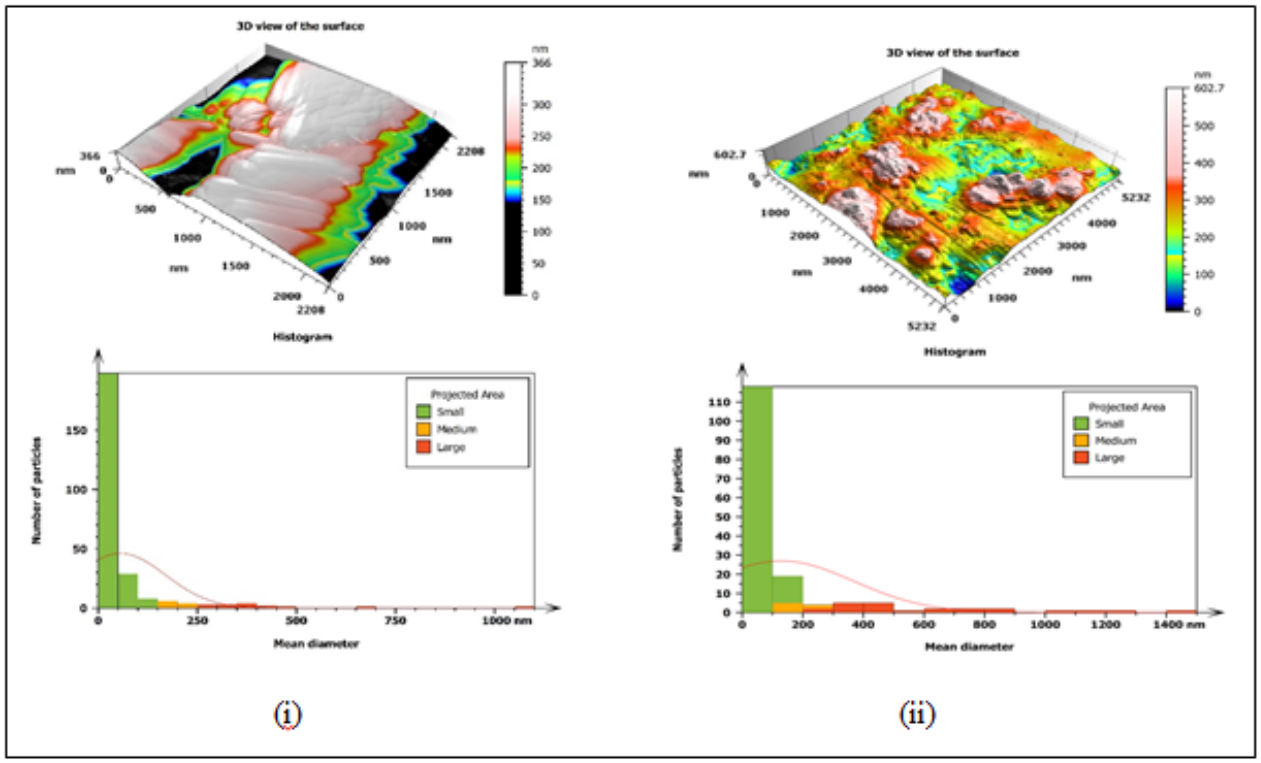

Figure 6 Report of particle distributions for corroded surface (i) and inhibited surface (ii) for Samafed drug.

3.2.Theoretical calculations

The first calculations that could be performed in the field of inhibition are related to the adsorption isotherm, using different relationships such as Langmuir, Langmuir-Freundlich and others. The Langmuir model is the most widely used. It analyzes the inhibition behavior by replicating each water molecule adsorbed by each drug molecule on the surface of a carbon steel. Figure (7) Illustrates the Langmuir relationship, represented by equation (3). A linear behavior is observed with a regression coefficient (R^2) close to unity. Samafed drug the relation between (C_{Drug}) and (C_{Drug}/θ) with (R^2) close to unity, where recorded (0.9995), (0.9912), (0.9853) and (0.9936) at (303) K, (313) K, (323) K and (333) K respectively, suggesting that Samafed drug as an inhibitor obeys the Langmuir isotherm theory .i.e., each adsorbed H_2O molecule will replace by $Samafed$ drug molecule. The calculated values for the adsorption-desorption constant are shown in Table (2), suggesting a physical adsorption of the Samafed drug, carried out by the Van der Waal interaction between the metal surface and the drug components by the functional groups suggested in the FTIR spectra. This adsorption also presents negative values ΔG^o_{ads} according to equation (4). The adsorption entropy is estimated from the relationship in equation (5) as shown in Figure (8) to give the negative entropy values refer to the role of activated complex ($Fe\ ion - Samafed\ drug$) in association rather than dissociative nature in reducing the ion movement on the surface, the entropy change refers to the difference between the entropy of corroded state and inhibited state ($S_{inhibited\ state} - S_{corroded\ state}$). Finally, the calculation of enthalpy results gave negative values which indicate the exothermic nature of adsorption i.e. the facility of adsorption of Samafed components.

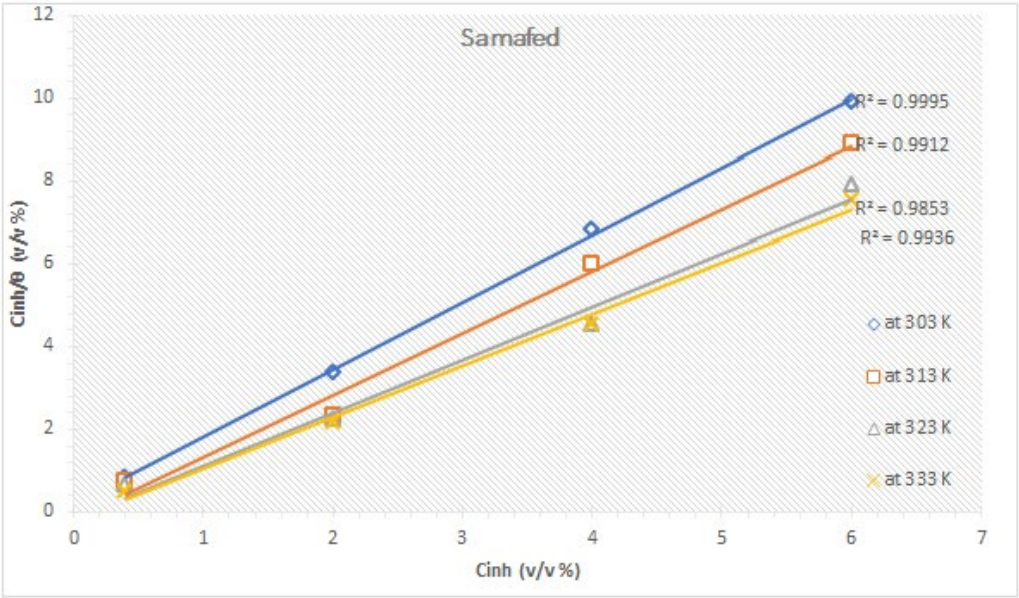

Figure 7 Langmuir relationship for the adsorption of Samafed drug.

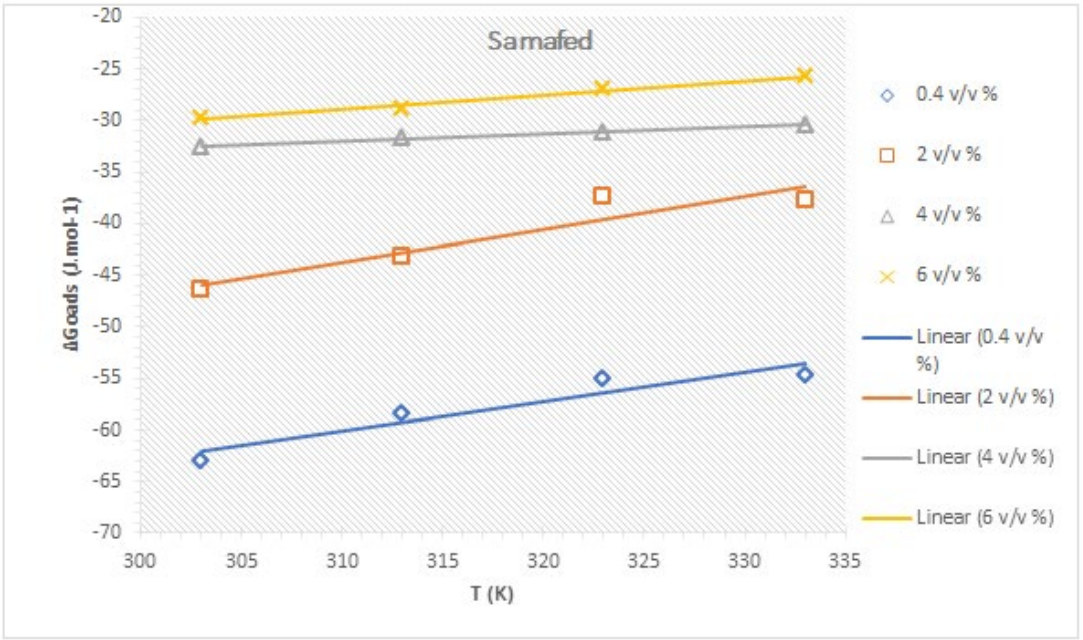

Figure 8 The relation between the changes in Gibbs energy (ΔG^{o}_{ads}) respected to temperature (T) for Samafed drug.

Table 2 Isotherm data of inhibition by Samafed drug.

Conc. (V/V %)	Temp. (K)	K_{ads} L/moL	ΔG^{o}_{ads} J/mole	ΔS^{o}_{ads} J/mole.K	ΔH^{o}_{ads} J/mole
0.4	303	35.26349977	-63.02508482	0.281421	22.24056
	313	20.0560536	-58.33250459		
	323	13.55697656	-55.0759082		
	333	13.00446698	-54.72991381		
2	303	4.764018645	-46.37947941	0.320676	50.78513
	313	3.261024765	-43.22748923		
	323	1.608860961	-37.35246474		
	333	1.667189709	-37.64860415		
4	303	0.89873064	-32.51036381	0.066434	-12.38067
	313	0.810914814	-31.65536132		
	323	0.764263917	-31.16266939		
	333	0.702345087	-30.46010701		
6	303	0.647041689	-29.77811863	0.140684	12.84756
	313	0.575804781	-28.80818193		
	323	0.460801143	-26.95547155		
	333	0.39652254	-25.70620348		

The calculation of electronic properties is a valuable tool to describe the nature of molecules through the energies of all atoms and groups in the structure. To study these properties by ($TD-DFT$) method two components of the drug Samafed, namely Pseudoephedrine and Triprolidine, are chosen, which have the optimized geometry shown in Figure (9); the electronic energy values are calculated according to different formulas listed in the experimental section and presented in Tables (3) and (4). Figure (9) Shows the atoms in different colors, including red for oxygen and blue for nitrogen. The Frontier molecule orbital densities of the two components of the drug Samafed are shown in Figure (10). They indicate the ability of the inhibitor to donate electrons through *HOMO* energy, which determines a high affinity (*Donor*) with a high value, while the *LUMO* energy informs us about the ability of the alloy to capture electrons (*Acceptor*) [46]. The energy gap in Table (3) related to ($\Delta E = E_{LUMO} - E_{HOMO}$) and its lower values indicate an excellent inhibitory effectiveness of the component [47]. Here can be seen that Triprolidine is the best because of having smallest energy gap (4.208eV) as illustrated in Figure (10). the negative value for $HOMO$ and $LUMO$ refer to the stable nature for components of drug. According to the principle of Hardness (η) and Softness (σ), low basicity and low electron donating ability refer to complex molecules, while high basicity and high electron donating ability refer to soft molecules [48], Therefore, the inhibitory activity increases with increasing softness (σ) and decreases with increasing hardness of the inhibitor molecules. According to the data in Table (4), both components present similar hardness and softness values. Furthermore, these properties (η andσ) are related to the stability and reactivity of the studied molecules [41]. A high value of the energy gap (ΔE) reflects the complex nature of the molecule, while a low value indicates its soft nature [42]. Therefore, Pseudoephedrine (5.883 eV) is a harder molecule than Triprolidine (4.208 eV), but both molecules act as inhibitors. However, the electronegativity values (χ) confirm the inhibitory activity of the Samafed drug components. Chemical potential (μ) is a measure of the potential energy of the molecule and a more negative value indicates a greater tendency to react or release energy and from table (4) it can be seen that Pseudoephedrine has the most negative value (-3.1085 eV). Electrophilicity (ω) measures the ability of a molecule (or atom) to attract electrons in a chemical bond. According to table (4), the Triprolidine molecule has the highest value (2.1615). The electron fraction (ΔN) is related to the number of electrons transferable to the acceptor molecule [49], represents the number of transferred electrons, which gave the highest value for the Triprolidine

molecule (0.9465). Finally, the dipole moment (D) describes the active sites in a molecule that give it the ability to interact with a metal surface (Metal or Alloy) [50]. In Figure (9), multiple active sites for drug components can be seen. The representation of molecules with molecular electrostatic potential (MEP) can be seen in Figure (11), where the red colored regions refer to the electron-rich sites (i.e. O, N) which have a source of lone electron pairs, and the blue colored regions refer to the electron-poor sites (i.e. alkyl groups and nucleophiles) and the effect of net electrostatic potential can be observed at a point in space surrounding a molecule with a total charge distribution ($electron + nuclei$) [51, 52]. In Figure (11), it can be seen that pseudoephedrine has many electrophilic groups, the surface pattern of *MEP* is -7.289e−2 *a.u.* (red) to +7.289e−2 *a.u.* (blue) [53-57].

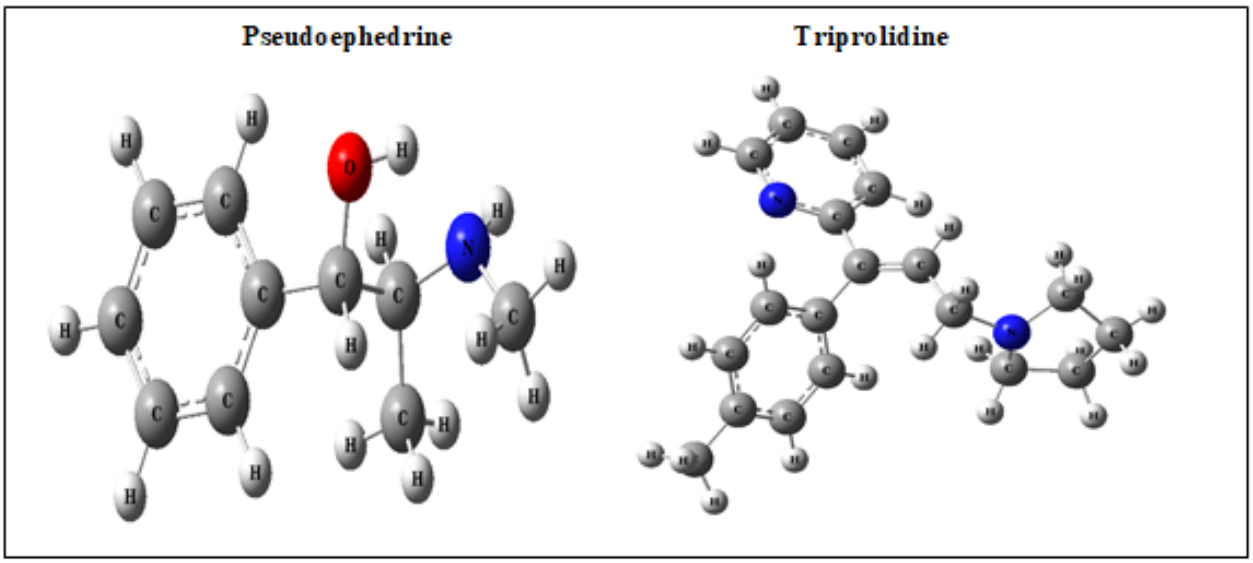

Figure 9 $B3LYP/6-31G$ Optimized geometries of (Samafed).

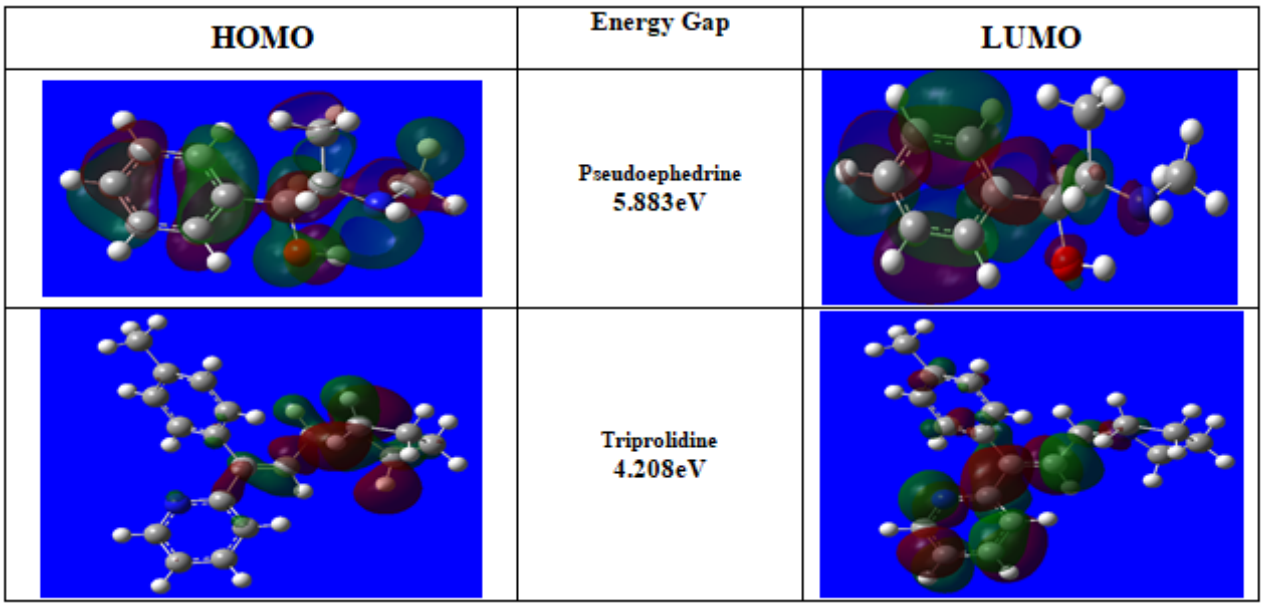

Figure 10 B3LYP/6-31G HOMO and LUMO of (Samafed).

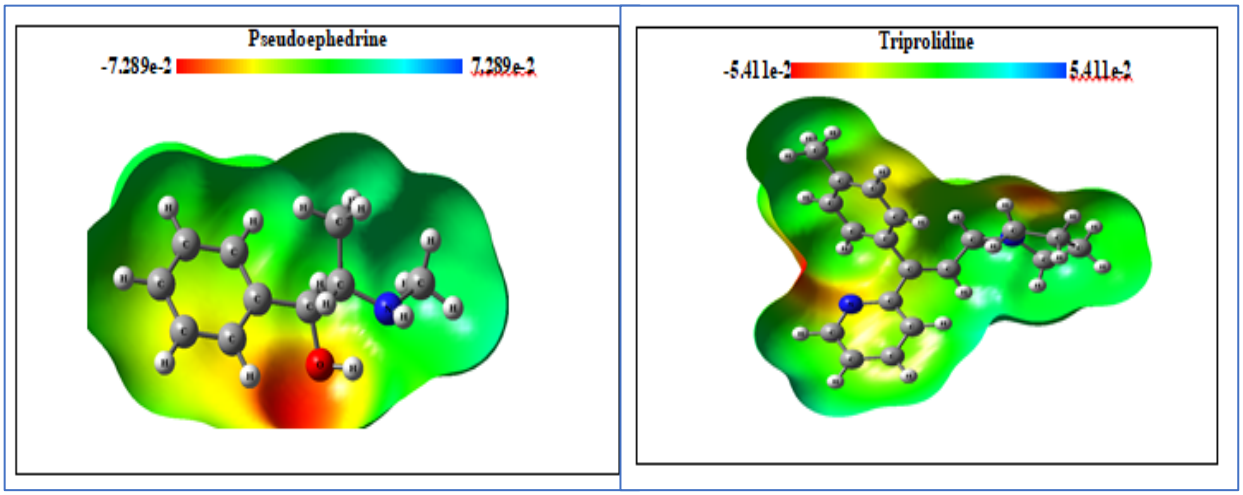

Figure 11 Molecular electrostatic potentials (MEP) of (Samafed).

Table 3 The energy properties for (Samafed) with the DFT at the B3LYP/6-311G level.

Component	**Total Energy (a.u.)**	E_{HOMO} **(eV)**	E_{LuMO} **(eV)**	**Energy gap (eV)**
Pseudoephedrine	-519.9236	-6.0501	-0.1670	5.883
Triprolidine	-846.5295	-5.1206	-0.9118	**4.208**

Table 4 The electronic properties for (Samafed) with the DFT.

(eV) Component	η	σ	χ	$-\mu$	ω	**ΔN**	D
Pseudoephedrine	2.9415	0.1699	3.1085	**-3.1085**	1.6424	0.6614	3.6324
Triprolidine	2.1044	0.2375	3.0162	-3.0162	**2.1615**	**0.9465**	2.1834

The surface characterization results obtained from SEM and AFM analyses confirm the formation of a protective layer at the nanoscale. AFM measurements, in particular, revealed significant changes in surface roughness and particle size distribution, indicating the development of a nanostructured film on the steel surface. The reduction in surface roughness from 270.8 nm to 90.77 nm demonstrates the effectiveness of the inhibitor in forming a uniform nanoscale protective layer. Table 5 presents the quantitative surface roughness, particle size distribution, and volume parameters obtained from AFM analysis for both corroded and inhibited samples, clearly showing the improvement in surface characteristics after inhibition. Furthermore, the increase in particle size and the reduction in pit and void volumes suggest improved surface coverage due to nanoscale adsorption of the drug molecules. These findings highlight the important role of nanotechnology concepts in understanding the inhibition mechanism, where the formation of a compact nanolayer acts as a barrier against corrosive ions.

Table 5 Surface roughness, particle size, and volume parameters obtained from AFM analysis for corroded and inhibited carbon steel surfaces.

Sample Condition	Surface Roughness (nm)	Mean Particle Diameter (nm)	Void Volume (nm^3)	Pit Volume (nm^3)
Corroded Surface	270.8	56.42	378.8	44.70
Inhibited Surface (Samafed, 2 v/v%)	90.77	128.0	159.0	8.869

4. CONCLUSIONS

The expired drug Samafed was used as a corrosion inhibitor for carbon steel in seawater, and its inhibitory activity was demonstrated by electrochemical measurements. Surface characterization using scanning electron microscopy and atomic force microscopy confirmed good surface coverage by the inhibitor. These analyses also revealed the formation of a uniform protective layer at the nanoscale, which plays a key role in reducing corrosion activity. Infrared spectroscopy tests revealed the presence of functional groups in the drug compound involved in the adsorption process, which was found to be predominantly physical in nature according to isothermal calculations. This adsorption process contributes to the formation of a thin nanolayer on the metal surface, enhancing the barrier properties against corrosive species. Further calculations were performed using quantum chemistry principles to confirm the inhibitory properties of the drug components. The electronic properties indicated the presence of active centers capable of interacting with the steel surface. These interactions occur at the molecular and nanoscale levels, supporting the stability and effectiveness of the protective film. The results suggest that Samafed acts as an effective corrosion inhibitor under the current experimental conditions, and the study highlights the importance of nanotechnology concepts in understanding the inhibition mechanism through nanoscale adsorption and surface film formation.

References

[1] Ansam A. Hashim, Rana A. Anaee and Mohammed s. Nasr, sustainable Chemistry and pharmacy, 44 (2025) 101905 https://doi.org/10.1016/j.scp.2025.101985
[2] Ansam A. Hashim, Rana Anaee and Mohammed S. Nasr, Ceramics 8 (2025) 11 https://doi.org/10.3390/ceramics8010011
[3] N. Patni, S. Agarwal, P. Shah, Chinese Journal of Engineering, 1 (2013) 1 https://doi.org/10.1155/2013/784186.
[4] P. B. Raja et al., Chemical Engineering Communications, 203 (2016) 1145 https://doi.org/10.1080/00986445.2016.1172485
[5] A. Y. El-Etre, M. Abdallah, Z. E. El-Tantawy, Corrosion Science 47 (2005) 385 https://doi.org/10.1016/j.corsci.2004.06.006
[6] E. E. Oguzie, Y. Liu, S. G. Wang, F. Wang, RSC Advances 1 (2011) 866 https://doi.org/10.1039/c1ra00148e
[7] Saja Abdul Maged, Rana Anaee M.T. Mathew, Journal of Bio- and Tribo-Corrosion, 1 (2023) 9 https://doi.org/10.1007/s40735-023-00786-1
[8] Ahmed Al-Ghaban, Hiba Abdullah, Rana Anaee, Shaimaa Naser, Anees Khadom, Journal of Engineering Research, 1 (2023) 23 https://doi.org/10.1016/j.jer.2023.11.020
[9] W. J. Lorenz, F. Mansfeld, Electrochimica Acta, 31 (1986) 467 https://doi.org/10.1016/0013-4686(86)80111-6
[10] M. M. Antonijević, Marija Petrović, International Journal of Electrochemical Science 3 (2008) 1 https://doi.org/10.1016/s1452-3981(23)15441-1
[11] N. Khalil, Electrochimica Acta 48 (2003) 2635 https://doi.org/10.1016/s0013-4686(03)00307-4
[12] T. A. Söylev and M. G. Richardson, Construction and Building Materials 22 (2008) 609 https://doi.org/10.1016/j.conbuildmat.2006.10.013
[13] Nnabuk O. Eddy, Stanislav R. Stoyanov and Eno E. Ebenso, Int. J. Electrochem. Sci, 5 (2010) 1127 https://doi.org/10.1016/S1452-3981(23)15350-8
[14] O. L. Riggs and R. M. Hurd, Corrosion 23 (1967) 252 https://doi.org/10.5006/0010-9312-23.8.252
[15] H. K. Aity, E. Dhahri, M. Rasheed, Ceram. Int. 111 (2024) 457 https://doi.org/10.1016/j.ceramint.2024.10.324

[16] Imran Naqvi, A.R. Saleemi and S. Naveed, Int. J. Electrochem. Sci, 6 (2011) 146 https://doi.org/10.1016/S1452-3981(23)14982-0
[17] F. Boudou, et al., Not. Sci. Biol. 17 (2025) 12593 https://doi.org/10.55779/nsb17312593
[18] N. Assoudi, et al., Opt. Quantum Electron. 54 (2022) 3927 https://doi.org/10.1007/s11082-022-03927-x
[19] F. Boudou, A. Guendouzi, A. Belkredar, M. Rasheed, Not. Sci. Biol. 16 (2024) 13837 https://doi.org/10.55779/nsb16211837
[20] A.J. Hussein, M.N. Al-Darraji, M. Rasheed, M.A. Sarhan, IOP Conf. Ser.: Earth Environ. Sci. 1262 (2023) 022005 https://doi.org/10.1088/1755-1315/1262/2/022005
[21] M. Darraji, L. Saqban, T. Mutar, M. Rasheed, A. Hussein, J. Adv. Biotechnol. Exp. Ther. 6 (2022) 687 https://doi.org/10.5455/jabet.2022.d147
[22] A.J. Hussein, M.N. Al-Darraji, M. Rasheed, IOP Conf. Ser.: Earth Environ. Sci. 1262 (2023) 022007 https://doi.org/10.1088/1755-1315/1262/2/022007
[23] T. Saidani, M. Rasheed, I. Alshalal, A.A. Rashed, M.A. Sarhan, R. Barillé, Res. Eng. Struct. Mater. 10 (2023) 743 https://doi.org/10.17515/resm2023.21ma0922rs
[24] Priyanka Singh, Deere Singh Chauhan, Kritika Srivastava, Vandana Srivastava, M. A. Quraishi, Int. J. Ind. Chem, 10 (2016) 017 10.22192/ijcrcps.2016.03.12.001
[25] Rana Afif Anaee, Ivan Hameed R. Tomi, Majid Hameed Abdulmajeed, Shaimaa Alaa Naser, Mustafa Mohammed Kathem, Journal of Molecular Liquids 279 (2019) 594 https://doi.org/10.1016/j.molliq.2019.01.169
[26] Rana Afif Anaee, Majed Hameed Abd Al-Majeed, Shaimaa Alaa Naser, Mustafa M. Kathem, and Omer Akram Ahmed, Al-Khwarizmi Engineering Journal 15 (2019) 71 https://doi.org/10.22153/kej.2019.08.002
[27] Rana Anaee, Haydar Aljaafari, Shaimaa Naser, Anees Khadom, Ali Abd and Tamara Anai, Iranian Journal of Chemistry and Chemical Engineering, Articles in Press (2025) https://doi.org/10.30492/ijcce.2025.2044014.6856.
[28] Akram Mohsin kadhim, Rana Afif Anaee, Mohammed Jasim M. Hassan, Munaf Adnan Idan Al-lami, Al-Mustansiriyah Journal of Science, 34 (2023) 33 http://doi.org/10.23851/mjs.v34i3.1335
[29] Shams A. Naji, Rana Afif Anee and Sadeer M. Majeed, Journal of Applied Sciences and Nanotechnology 4 (2024) 47 https://doi.org/10.53293/jasn.2024.7485.1314
[30] Saja A. Abdul Maged, Rana A. Anaee, Mathew T. Mathew, AIP Conf. Proc. 3169 (2025) 040108 https://doi.org/10.1063/5.0254307
[31] Rana A. Anaee, Asian Journal of Chemistry, 26 (2014) 4469 https://doi.org/10.1253/5.0254245
[32] Hiba A. Abdullah, Rana A. Anaee, Anees A. Khadom, Ali T. Abd Ali, Aya H. Malik, Mustafa M. Kadhim, Results in Chemistry 6 (2023) 101035 https://doi.org/10.1016/j.rechem.2023.101035
[33] Sh. A. Naser, R. A. Anaee and H. A. Jaber, Advances in Materials and Processing Technologies 55 (2024) 647 https://doi.org/10.1080/2374068X.2024.2306568
[34] Sh. Naser, R. Anaee and H. Jaber, Chemistry Africa 44 (2023) 25 https://doi.org/10.1007/s42250-023-00838-6
[35] N. Najm, A. H. Ataiwi and R. A. Anaee, Materials Today: Proceeding 62 (2022) 4551 https://doi.org/10.1016/j.matpr.2022.05.241
[36] R. A. Anaee, Journal of Bio- and Tribocorrosion 2 (2016) 257 10.1007/s40735-016-0036-1
[37] H. A. Abdullah, R. A. Anaee, A. A. Khadom, A. T. Abd Ali, A. H. Malik, M. M. Kadhim, Results in Chemistry 6 (2023) 101035 https://doi.org/10.1016/j.rechem.2023.101035
[38] Hiba A. Abdulaah, Ahmed M. Al-Ghaban1, Rana A. Anaee, Anees A. Khadom and Mustafa M. Kadhim, J. Electrochem. Sci. Eng. 13 (2023) 115 https://doi.org/10.5599/jese.1257
[39] M. H. Hafiz, R. A. Anaee, R. S. Noor, M. A. Wehib, Int. J. Electrochem. Sci. 8 (2013) 12402 https://doi.org/10.1016/S1452-3981(23)13276-7
[40] F. Boudou, A. Belkredar, A. Berkane, M. Rasheed, Not. Sci. Biol. 17 (2025) 12183 https://doi.org/10.55779/nsb17212183
[41] A. A. Issa and H. R. Obayes, J. Mol. Model. 26 (2020) 10 10.1007/s00894-020-04558-3

[42] A. A. Issa, M. D. Kamel, and D. S. El-Sayed, J. Mol. Model. 30 (2024) 106 10.1007/s00894-024-05896-2
[43] W. J. Pietro, M. M. Franc, W. J. Hehre, D. J. Defrees, J. A. Pople, J. S. Binkley, Journal of the American Chemical Society 104 (1982) 5039 10.1021/ja00383a007
[44] K. D. Dobbs and W. J. Hehre, Journal of Computational Chemistry 8 (1987) 861 10.1002/jcc.540080614
[45] Ahmad H. Ismail, Hassanain K. Al-Bairmani, Zainab S. Abbas, Ahmed M. Rheima, Nano Biomed. Eng., 12 (2020) 139 10.5101/nbe.v12i2.p139-147
[46] P. Nikhil, M. L. Yuri, L. Ning, H. S. Jan and M. Melgardt, Pharmaceutical Research 22 (2005) 826 10.1007/s11095-005-2600-0
[47] H. Ibraheem, Y. Al-Majedy, A. A. Issa, and E. Yousif, Trends Sci. 21 (2023) 7374 10.48048/tis.2024.7374
[48] A. A. Issa, H. H. Ibraheem, and D. S. El-Sayed, J. Mol. Model. 30 (2024) 14 10.1007/s00894-023-05815-x
[49] Y. K. Al-Majedy, H. H. Ibraheem, and A. A. Issa, AIP Conf. Proc. 2593 (2023) 1245 10.1063/5.0113038
[50] H. H. Ibraheem, A. A. Issa, and D. S. El-Sayed, J. Mol. Struct. 1312 (2024) 138484 10.1016/j.molstruc.2024.138484
[51] P. G. Magar, R. Uprety and K. B. Rai, Him. Phys. 11 (2024) 28 https://doi.org/10.3126/hp.v11i1.65329
[52] M. I. Sayyed, K. M. Kaky and R. A. Anaee, Journal of Theoretical and Applied Physics 17 (2020) 172355 https://dx.doi.org/10.57647/j.jtap.2023.1705.55
[53] Z. S. Ahmed, M. RASHEED, H. S. Ahmed, Experimental and Theoretical NANOTECHNOLOGY 10 (2026) 329 https://doi.org/10.56053/10.s.329
[54] Z. S. Ahmed, M. RASHEED, H. S. Ahmed, Experimental and Theoretical NANOTECHNOLOGY 10 (2026) 343 https://doi.org/10.56053/10.s.343
[55] A. Khaleefah, M. RASHEED, Experimental and Theoretical NANOTECHNOLOGY 10 (2026) 289 https://doi.org/10.56053/10.s.289
[56] A. I. A. Ali, M. RASHEED, Experimental and Theoretical NANOTECHNOLOGY 10 (2026) 277 https://doi.org/10.56053/10.s.277
[57] A. I. A. Ali, M. RASHEED, Experimental and Theoretical NANOTECHNOLOGY 10 (2026) 239 https://doi.org/10.56053/10.s.239